

Geochemical studies of the gold mineralization of Kodiarani-(Doko permit). Prefecture of Siguiri, Administrative region of Kankan, Republic of Guinea

Soryba BANGOURA ^{1,*}, Kandas KEITA ², Mamadou Oury DIALLO ¹ and Abdoulaye Kadiatou DIALLO ¹

¹ Department of geological services, Higher Institute of Mines and Geology of Boké, Rep. of Guinea.

² Department of Processing-Metallurgy, Higher Institute of Mines and Geology of Boké, Rep. of Guinea.

World Journal of Advanced Research and Reviews, 2023, 20(01), 1123–1138

Publication history: Received on 13 September 2023; revised on 24 October 2023; accepted on 27 October 2023

Article DOI: <https://doi.org/10.30574/wjarr.2023.20.1.2151>

Abstract

West Africa is now a major player in world gold production with numerous gold deposits hosted in Birimien green belts (2.2-2.0 Ga). However, these belts and their geological formations remain unexplored, as does their evolution during the Eburnean orogeny. This is why, after acquiring its exploration Licence, TOROGOLD focused its work on Air Core drilling activities in the Doko-Kodiarani Licence in north-eastern Guinea. During these activities, geochemical studies will be carried out on rock samples taken from the six (6) boreholes pre-selected for this purpose.

The aim of this research work is to carry out a geological study in order to determine the chemical associations between the mineralization, the nature of the host rock and others for future work. To achieve this objective, we used a number of methods, including a statistical approach, field reconnaissance, and macroscopic and litho-geochemical analyses. Geochemical studies reveal that the rocks studied are meta-sediments. They belong to the schist groups. Their protholites are moderately altered ($60 < CIA < 80$) and the source is thought to be andesitic and basaltic, emplaced in a geotectonic oceanic island arc. As for the various AC drilling sections, our observations reveal that the gold mineralization is found in two types of deposit: disseminated, present in all lithology's, and vein-type, resulting from the filling of fracture zones, associated with the highest concentrations. We noted a strong discontinuity of mineralization in these veins, due to a tectonic phase that may have played an important role in the remobilization of gold in these structures.

Keywords: Birimien; Litho geochemistry; Protholites; Mineralization; Tectonic

1. Introduction

At a time when the mining industry plays a key role in the development of nations, mineral raw materials such as gold, iron, uranium, ... are increasingly sought after [1].

Like other great nations, Guinea has immense agricultural, hydraulic and energy potential, as well as numerous world-class mining resources such as bauxite, iron and precious metals, including gold (estimated reserves of around 700 tonnes [1, 2, 3, 4]). As a mining country, the Republic of Guinea is the eighth largest gold producer in Africa and the third largest in the world in 2019, with production of 27.5 tonnes/year. These deposits are generally located in Upper Guinea and in certain localities in Lower and Middle Guinea [1]. From a global perspective, gold mining contributes to the country's economic development by reducing unemployment and creating jobs, but it also has a negative impact on the environment, particularly by polluting water resources [5].

* Corresponding author: Soryba BANGOURA

A number of mining exploration permits have been awarded to mining companies for the exploration of precious metals, including gold, and base metals. TOROGOLD (a subsidiary of the RESOLUTE MINING Group) applied for and obtained a gold exploration Licence in Upper Guinea (Doko Licence) in the Siguiri basin, more specifically in the sub-prefecture of Doko (Siguiri prefecture) [6, 7, 8].

Since obtaining this Licence, TOROGOLD has carried out a number of exploration activities in accordance with its mining research protocol, including soil geochemistry, mapping and a series of drill holes (Auger and Air Core). This work led to the identification of the Kodiarani prospect. It was with this in mind that we were able to make our modest contribution to the geochemical study using data from Air Core (AC) drilling and multi-element analysis (XRF) [7,8,9,10]. Mining, agricultural inputs and domestic waste are the main sources of pollution of water resources. However, the current challenge for the mining sector is to strike a balance between preserving the quality of the environment (groundwater and surface water) and reducing greenhouse gas emissions [10].

1.1. Geographical context

Siguiri is a prefecture in the administrative region of Kankan, located 761 km from the capital Conakry. Its geographical coordinates are 11°25'20" North and 9°10'11" West, with a surface area of 15,500 km² (fig. 1).

It is bounded

- To the north and east by the Republic of Mali,
- To the south by the Prefectures of Kankan and Kouroussa,
- To the south-east by the Prefecture of Mandiana,
- To the west by the Prefecture of Dinguiraye [9].

The prefecture of Siguiri has a population of 724,631 (2016 census), with an average density of 47 inhabitants per km².

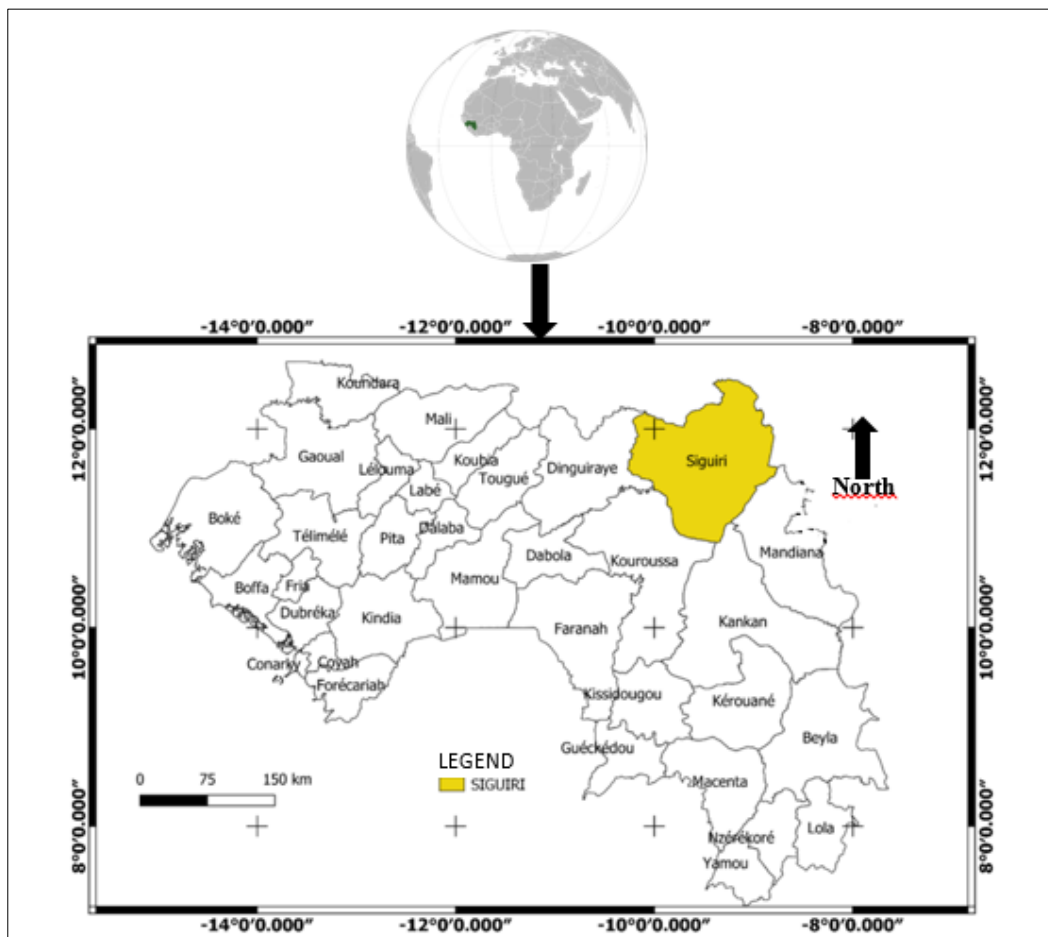


Figure 1 Administrative Map of Guinea

1.2. Geological context

1.2.1. The West African craton

From a geological point of view, the study area is located in the West African craton, which is one of the five (5) cratons of the basement that makes up the African plate (fig. 2). It is composed of Precambrian terrains that outcrop at the level of the Reguibat ridge to the north and the Man or Leo ridge to the south, formed by the Archean series of the Liberian shield and the Palaeoproterozoic formations of the Baoulé-Mossi domain covering Ghana, Côte d'Ivoire, Guinea, southern Mali, Burkina Faso and western Niger [11]. These Palaeoproterozoic formations are generally referred to as Birimien. The rest of the craton is covered by late Neoproterozoic sediments, which form the Taoudéni basin. The West African craton stabilized at around 1.7 Ga, although it still bears traces of more recent Orogenesis, particularly in its peripheral part [11, 12].

The West African Craton hosts numerous gold deposits hosted by formations of Palaeoproterozoic (Birimien) age and are orogenic deposits that formed during the Eburnean cycle, around 2 billion years ago [12].

According to [10], the study area consists of the Proterozoic formations (PR1 and PR2).

Lower Proterozoic (PR1)

Formed by sediments that constitute the dominant facies of the Siguiri basin. These are often finely stratified mudstones, siltstones and feldspathic sandstones, with intercalated banks of fine sandstones. Outcrops are also relatively numerous in the beds of small streams flowing at the foot of large isolated massifs [10, 11].

Upper Proterozoic (PR3)

This formation is widely exposed in the north-western part of the region, where it is intercalated between the Birimien basement and the basic rocks of the Mesozoic (gabbro's and dolerites). The Upper Proterozoic sandstones and conglomerates form the sub-horizontal entablatures bounded by cliffs that are clearly visible in the landscape. These cliffs represent the first step of the plateau that develop towards the Republic of Mali [11].

The study area belongs to the Guinea-Liberian shield of the West African platform.

There are two (2) structural levels:

- Lower structural stage or basement

The study region is made up of Lower Proterozoic formations that are deeply folded, metamorphosed and dislocated as a result of the tectonic movements that have affected the region. These movements led to the development of granitization within the Birimien formations [12, 13, 14].

- Upper structural layer or cover

Represented by the Guinea-Liberian shield, this stage is essentially made up of sub horizontal sedimentary rocks resting in angular discordance on the basement formations, which are: sandstones, terrigenous deposits and river alluvium [13].

1.2.2. Mineralization

Field work revealed two (2) types of mineralization: primary and secondary mineralization [14].

Primary mineralization

For this type of mineralization, SAG's work revealed 3 types:

- In-situ primary mineralization mainly associated with quartz veins, veinlets and stock-works identical to that recognized around the village of Kintinian;
- Mineralization associated with a volcanic breccia where gold-bearing quartz and sulphides fill fissures within the volcanic vent;
- Paleo-placers that are currently high up in relation to the watercourses, and which account for 70% of the deposit's reserves [13, 14, 15].

Secondary mineralization

These are alluvial deposits from river beds and existing terraces. They are found almost everywhere in the Siguiri Prefecture.

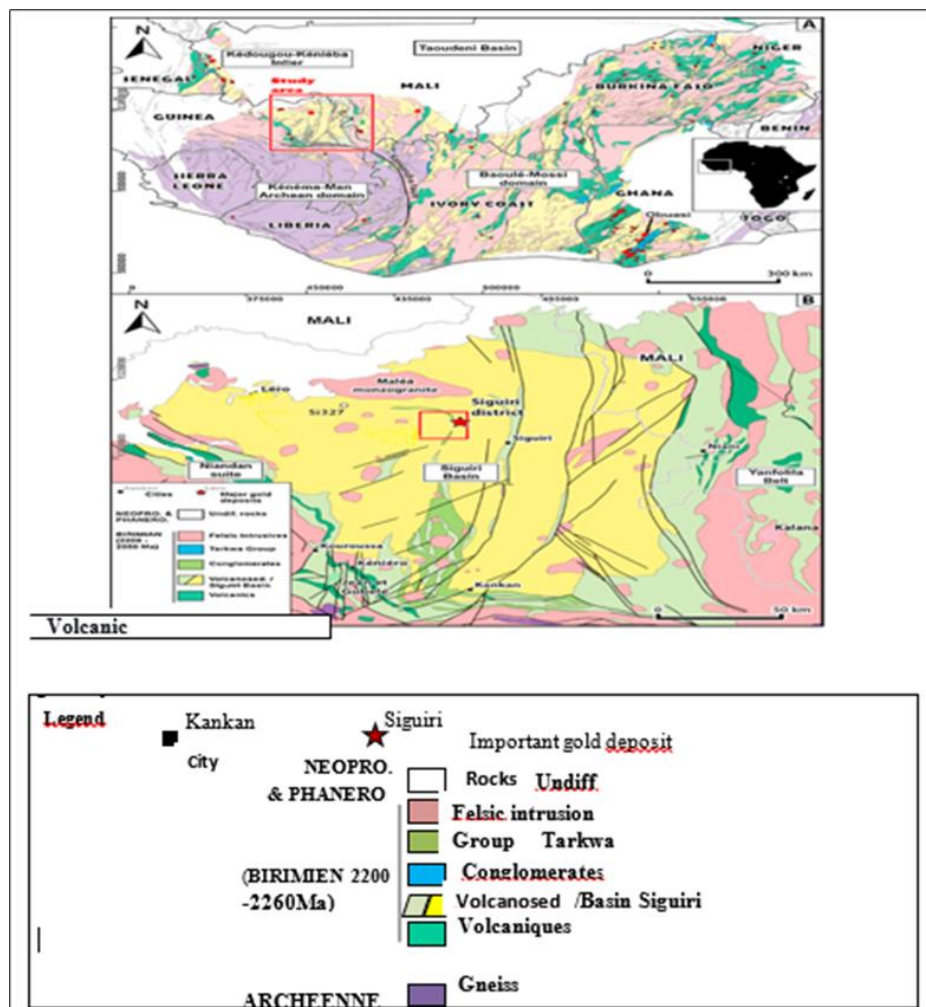


Figure 2 A: geological map of the West African craton; B: map of the Siguiri basin.

1.2.3. Geology of Kodiarani (Doko Licence)

The geology of our Licence (Fig. 3) is dominated by Birimien (Proterozoic) rocks composed mainly of turbidity-facies sedimentary sequences (derived from submarine movement), represented by argillites, sandstones and greywackes. Intrusive rocks are represented by granodiorites, which outcrop in the north-east and west, while dolerites, gabbro's and monzogranites outcrop in the south-west of the Licence area [13, 14, 15, 16]. Laterites and a few free angular quartz fragments can be found in certain parts of the region. The host rocks in the study area consist of basalts, andesite's and oxidized saprolites formed as a result of intense meteorite alteration at the surface.

Mineralization

According to [14, 15, 16], studies carried out on the Doko Licence have revealed two types of mineralization:

- In situ mineralization: linked to quartz veins hosted in meta-sediments with mineralization occurring preferentially in siltstones and coarser, brittle sandstones in stock-werks.
- Saprolite mineralization: this type occurs in the zone when the underlying mineralized rocks have been deeply altered [16, 17, 18].

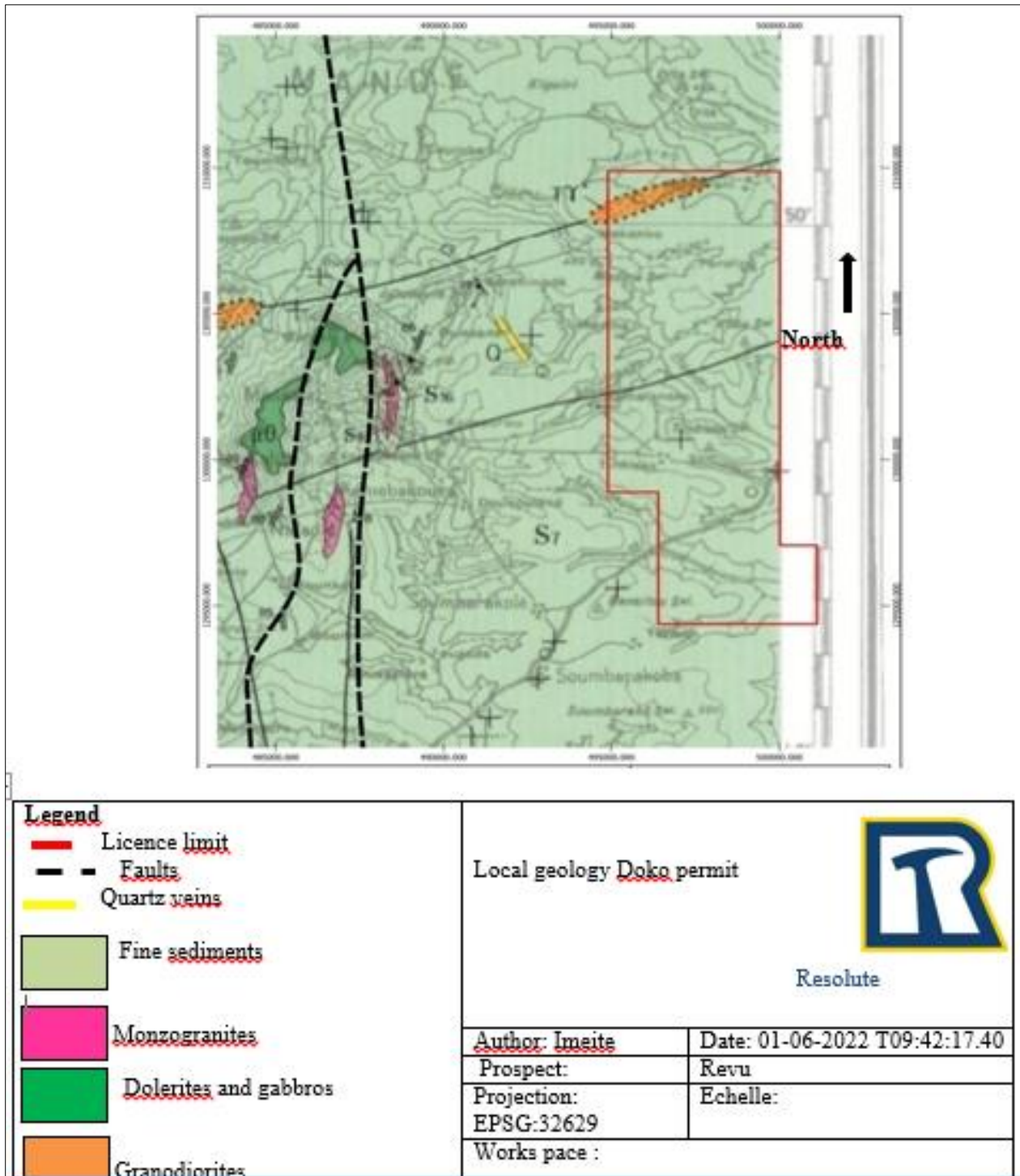


Figure 3 Geological map of Kodiarani-permit of Doko

2. Material and methods

Generally speaking, gold is one of the precious or noble metals whose content in the earth's crust is very low, around 5.10-7% or 0.005 ppm. It can be found in its native state or associated with other minerals (Table 1).

Table 1 Economic minerals of gold

Name	Formula	% Au	Density g/cm ³	Colour
Gold	AU	100	15-19.5	Golden yellow
Electrum	Au,Ag	55-80	12.5-15.5	Pale yellow
Maldonite	Au ₂ Bi	65	15.5	Orange-white
Calaverite	(Au, Ag) Te ₂	39.,5-44	9-9.5	Bronze-yellow
Crennerite	(Au, Ag) Te ₂	39.5	8.35	Yellowish white
Sylvanite	(Au, Ag) Te ₄	24.5	7.9-8.3	Steel-grey
Petzite	(Au, Ag) ₂ Te	12-25	8.7-9	Grey-black
Hagyagite	Au ₂ Pb ₁₄ Sb ₃ Te ₇ S ₁₇	6-13	7	Lead-grey

2.1. Physical aspect

Gold has the chemical symbol (Au) and occupies 79th place in the Mendeleev periodic table. It belongs to group eleven [11], which includes copper and silver, with an atomic mass of 196.97, density 19.3g/cm³, melting point 1064°C and boiling point 2960°C. Gold is the most ductile of metals, and can be rolled into sheets up to 0.0001mm thick. A good conductor of heat and electricity (2nd behind silver) Gold has the chemical symbol (Au) and occupies 79th place in Mendeleev's periodic table. It belongs to group eleven [11], which includes copper and silver, with an atomic mass of 196.97, density 19.3g/cm³, melting point 1064°C and boiling point 2960°C. Gold is the most ductile of metals, and can be rolled into sheets up to 0.0001mm thick. A good conductor of heat and electricity (2nd behind silver) Gold has the chemical symbol (Au) and occupies 79th place in Mendeleev's periodic table. It belongs to group eleven [11], which includes copper and silver, with an atomic mass of 196.97, density 19.3g/cm³, melting point 1064°C and boiling point 2960°C. Gold is the most ductile of metals, and can be rolled into sheets up to 0.0001mm thick. A good conductor of heat and electricity (2nd only to silver).

2.2. Chemical aspect

A metal that oxidizes with difficulty and is chemically very resistant; it is not attacked by oxygen or strong acids, dissolves in aqua regia and cyanide, and is soluble in mercury (amalgamation). During field work, the main equipment used to take Air Core samples was as follows:

- **The Air Core drill:** It allows us to drill boreholes in order to obtain representative samples. It consists of a double-entry rod. The first (external), is used to send compressed air which acts on the spoil removed by the hammer and the second (internal) allows the spoil to rise to the surface to be recovered by an instrument attached to the mast of the drill by pipes (connectors) called a cyclone [17].
- **The cyclone:** Is a cyclic polygonal instrument used to recover rock cuttings from the drill using **large plastics**.
- **The divider:** This is used to mix and reduce the excavated material to obtain an optimum 2.5 kg sample for laboratory analysis [19].

**Figure 4** Air core drill

The materials for the lithochemical study came from:

- Borehole data: obtained by observation and macroscopic description of the samples taken from the borehole (Fig. 5), to be processed and interpreted:
- Borehole data: obtained by observation and macroscopic description of the samples taken from the borehole (Fig. 5), to be processed and interpreted.



Figure 5 Chip-tray, containing rock fragments

Geochemical data: These are results obtained from laboratory analyses of the concentration of one or more elements (metals, major, minor and trace elements) in samples [19].

XRF results data: These are the results of analyses obtained from the XRF device.

- The XRF apparatus: Is an analytical tool for obtaining quantitative analyses of the chemical elements contained in a sample. From the major, minor and trace elements in fresh rocks, it can also determine the nature of the rocks in a geological formation. The XRF analysis process is divided into the following stages:
- Emission: This consists of emitting photons that bombard the sample from the X-ray tube.
- Excitation: The X-ray emitted strikes the elements contained in the samples, which in turn emit a fluorescence that returns to the analyzer's X-ray detector [20].
- Measurement: The detector measures the energy spectrum. The energies detected tell the analyzer which elements are present in the sample and in what quantities. It processes the energy spectrum and displays the elemental composition of the sample analyzed. The results extracted from the spectrum are expressed in % or ppm (g/t) [20, 21].

3. Results and discussion

Generally speaking, the lithochemical study of gold mineralization at the Kodiarani prospect based on the AC drilling samples, combined with the documentary research related to the same objectives, have enabled us to obtain results for interpretation purposes. Interpretation of these results will enable us to give an opinion not only on the origin of the mineralization, but also on the zonation's that host it, with a view to guiding future work.

3.1. Results Lithologiques

To begin with, we carried out a petrographic study based on macroscopic observations of the various samples collected in the field (chip-tray). This information was then entered into a log sheet-from AC-prepared by the company (Table 2). It shows the state of weathering, the lithology and the different stages of weathering encountered, as well as the percentage of quartz and sulphides fragments (pyrite, arsenopyrite).

Table 2 Logging sheet for hole DKAC0066

Hole_ID	Depth_From	Depth_To	Weathering	Oxidation	Regolith1	Lith1-Code-Description	ALT1-Code-Description	Min1-code-Description	Vein1_Code_Description	Vein1_Pct	Comments
DKAC0066	0	1	CW	OX	L	DLAT Lateritized	HE hematite	Pas de sulfure (pyrite, arsénopyrite)	VQZ Vein - Quartz	Varies from 2 to 20%	Quartz is oxidized with the presence of cavities
DKAC0066	1	2	CW	OX	L	DLAT Lateritized	HE hematite				
DKAC0066	2	3	CW	OX	L	DLAT Lateritized	HE hematite				
DKAC0066	3	4	CW	OX	L	DMOT Mottled Saprolite	HE hematite				
DKAC0066	4	5	CW	OX	MZ	DMOT Mottled Saprolite	HE hematite				
DKAC0066	5	6	CW	OX	MZ	XCY Saprolitic Clay	HE hematite				
DKAC0066	6	7	CW	OX	XU	XCY Saprolitic Clay	HE hematite				
DKAC0066	7	8	CW	OX	XU	XCY Saprolitic Clay	LM limonite				
DKAC0066	8	9	CW	OX	XU	XCY Saprolitic Clay	LM limonite				
DKAC0066	9	10	CW	OX	XU	SSL Siltstone	LM limonite				
DKAC0066	10	11	CW	OX	XU	SSL Siltstone	HE hematite				
DKAC0066	11	12	CW	OX	XU	SSL Siltstone	HE hematite				
DKAC0066	12	13	CW	OX	XU	SSL Siltstone	HE hematite				
DKAC0066	13	14	CW	OX	XU	SSL Siltstone	HE hematite				
DKAC0066	14	15	CW	OX	XU	SSL Siltstone	HE hematite				
DKAC0066	15	16	CW	OX	XU	SSL Siltstone	HE hematite				

DKAC0066	16	17	CW	OX	XU	SSL Siltstone	LM limonite				
DKAC0066	17	18	CW	OX	XU	SSL Siltstone	LM limonite				
DKAC0066	18	19	CW	OX	XU	SSL Siltstone	LM limonite				
DKAC0066	19	20	CW	OX	XU	SSL Siltstone	LM limonite				
DKAC0066	20	21	CW	OX	XU	SSL Siltstone	LM limonite				
DKAC0066	21	22	CW	OX	XU	SSL Siltstone	HE hematite				
DKAC0066	22	23	CW	OX	XU	SSL Siltstone	KO kaolinite - clay				
DKAC0066	23	24	CW	OX	XU	SSL Siltstone	KO kaolinite - clay				
DKAC0066	24	25	CW	OX	XU	SSL Siltstone	KO kaolinite - clay				
DKAC0066	25	26	CW	OX	XU	SSL Siltstone	KO kaolinite - clay				
DKAC0066	26	27	CW	OX	XU	SSL Siltstone	KO kaolinite - clay				
DKAC0066	27	28	CW	OX	XU	SSL Siltstone	KO kaolinite - clay				
DKAC0066	28	29	CW	OX	XU	SSL Siltstone	KO kaolinite - clay				
DKAC0066	29	30	CW	OX	XU	SSL Siltstone	KO kaolinite - clay				
DKAC0066	30	31	CW	OX	XU	SSL Siltstone	KO kaolinite - clay				
DKAC0066	31	32	CW	OX	XU	SSL Siltstone	KO kaolinite - clay				
DKAC0066	32	33	HW	OX	XL	SSL Siltstone	CH chlorite + calcite				
DKAC0066	33	34	HW	OX	XL	SSL Siltstone	CH chlorite + calcite				
DKAC0066	34	35	HW	OX	XL	SSL Siltstone	CH chlorite + calcite				

DKAC0066	35	36	HW	OX	XL	SSL Siltstone	CH chlorite + calcite				
DKAC0066	36	37	HW	OX	XL	SSL Siltstone	CH chlorite + calcite				
DKAC0066	37	38	HW	OX	XL	SSL Siltstone	CH chlorite + calcite				
DKAC0066	38	39	HW	OX	XL	SSL Siltstone	CH chlorite + calcite				
DKAC0066	39	40	HW	OX	XL	SSL Siltstone	CH chlorite + calcite				
DKAC0066	40	41	HW	OX	XL	SSL Siltstone	CH chlorite + calcite				
DKAC0066	41	42	HW	OX	XL	SSL Siltstone	CH chlorite + calcite				
DKAC0066	42	43	HW	OX	XL	SSL Siltstone	CH chlorite + calcite				
DKAC0066	43	44	HW	OX	XL	SSL Siltstone	CH chlorite + calcite				
DKAC0066	44	45	HW	OX	XL	SSL Siltstone	CH chlorite + calcite				
DKAC0066	45	46	HW	OX	XL	SSL Siltstone	CH chlorite + calcite				
DKAC0066	46	47	HW	OX	XL	SSL Siltstone	CH chlorite + calcite				
DKAC0066	47	48	HW	OX	XL	SSL Siltstone	CH chlorite + calcite				
DKAC0066	48	49	HW	OX	XL	SSL Siltstone	CH chlorite + calcite				
DKAC0066	49	50	HW	OX	XL	SSL Siltstone	CH chlorite + calcite				
DKAC0066	50	51	HW	OX	XL	SSL Siltstone	CH chlorite + calcite				
DKAC0066	51	52	HW	OX	XL	SST Sandstone (undif)	CH chlorite + calcite				
DKAC0066	52	53	HW	OX	XL	SST Sandstone (undif)	CH chlorite + calcite				
DKAC0066	53	54	MW	TR	XP	SST Sandstone (undif)	CH chlorite + calcite				
DKAC0066	54	55	MW	TR	XP	SST Sandstone (undif)	CH chlorite + calcite				
DKAC0066	55	56	MW	TR	XP	SST Sandstone (undif)	CH chlorite + calcite				

DKAC0066	56	57	MW	TR	XP	SST Sandstone (undif)	CH chlorite + calcite				
DKAC0066	57	58	MW	TR	XP		CH chlorite + calcite				

Secondly, we transferred the data from the table to a geological software package (Leapfrog) in order to make drill sections. Observation of the different sections obtained from these air-core drilling data reveals three main formations (Section in Fig. 6), from top to bottom: laterite, Saprolite and source rocks (sediments).

- Laterite (L): Reddish to brownish-red soil, rich in iron hydroxide, most often characterized by the presence of pisolites.
 - Mottled zone (MZ): Characterized by the disappearance of most of the primary textures and by the development of centimetric patches of iron oxides and hydroxides within the clay matrix.
- Saprolite (XCY): Heavily weathered rock in which the structure and primary texture of the parent rock have been preserved. It includes :
 - Upper Saprolite (XU): Or fine Saprolite is the water-saturated zone, marked by the predominance of secondary weathering minerals.
 - Lower Saprolite (XL): also known as coarse Saprolite, is a formation dominated by the nature of the parent rock, with fragments of rocks and primary minerals in separate grains.
- Sap rock (XP): Consisting of Silstones (SSL) and Sandstones (SST), it is characterized by a sandstone facies with a fine to coarse grain size, with varied colors due to alteration. It is the transition zone between Saprolite and fresh rock; it is generally compact and slightly weathered.

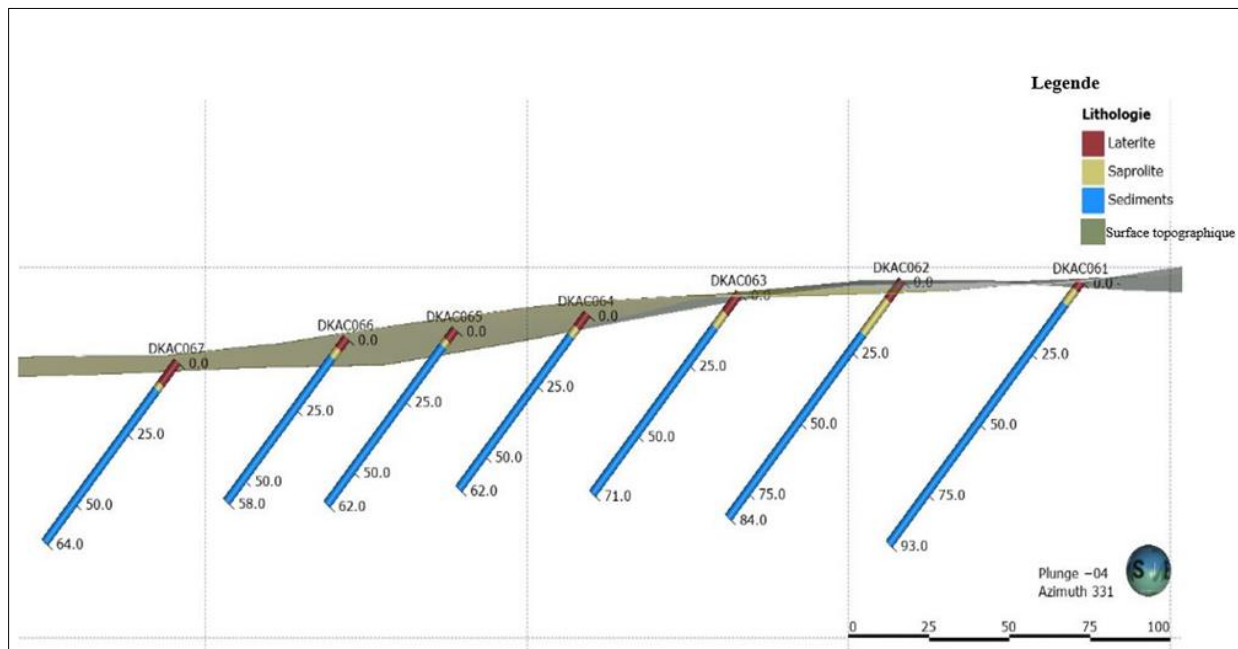


Figure 6 Sections of the three main formations

3.2. Geochemical Results

A total of 476 samples were analyzed by XRF to identify major and trace elements (in blue). These results are used to characterize the lithology’s from the samples. To exploit this database properly, we selected three (3) samples per borehole, between 50 and 80m depending on the depth of the borehole, in order to limit the effects of meteorite alteration [19, 20].

The different concentrations of major and trace elements are shown in Table 3. SiO₂ compositions range from 54.90 to 60.64%, with Al₂O₃ contents varying from 22.96 to 27.52%.

The Fe₂O₃ and MgO concentrations range from 5.49-10.54% and 0.25-4.20% respectively.

The CaO and TiO₂ compositions range from 0.00-0.57%, 0.80 and 0.99% respectively. The alkaline content of Na₂O and K₂O is between 2.96 et 8,08 and 8.08% and 0.50-2.62% respectively; TiO₂ is between 0.99-0.78% and P₂O₅ is 0.01%.

Table 3 Composition of major and trace chemical elements (%) in samples from the Doko Licence

Locality	Kodia rani	Kodia rani	Kodia rani	Kodia rani	Kodia rani	Kodia rani	Kodia rani	Kodia rani	Kodia rani	Kodia rani	Kodia rani
Samples	GR713 04	GR713 05	GR713 06	GR713 83	GR713 84	GR713 85	GR714 52	GR714 53	GR714 54	GR715 85	GR715 86
SiO ₂	60.64	58.72	58.06	55.54	54.90	58.72	52.46	59.20	55.46	55.32	54.34
Al ₂ O ₃	24.23	23.29	24.67	25.34	24.51	22.96	26.87	22.48	27.52	23.47	24.96
Fe ₂ O ₃	5.49	8.36	6.32	6.97	8.49	7.19	7.59	7.43	6.49	10.08	10.54
CaO	0.00	0.00	0.00	0.00	0.00	0.00	0.04	0.13	0.10	0.57	0.48
MgO	0.25	0.25	0.25	0.25	0.25	0.25	0.25	0.25	0.25	2.27	4.20
Na ₂ O	5.14	4.78	6.03	6.72	6.60	5.72	8.08	5.98	5.93	5.31	2.96
K ₂ O	1.67	1.99	2.07	2.49	2.62	2.27	2.13	1.88	1.68	0.50	0.60
TiO ₂	0.80	0.86	0.78	0.89	0.92	0.85	0.96	0.96	0.98	0.91	0.99
MnO	0.11	0.42	0.06	0.09	0.08	0.03	0.03	0.07	0.06	0.07	0.03
P ₂ O ₅	0.01	0.01	0.01	0.01	0.01	0.01	0.01	0.01	0.01	0.01	0.01
LOI	2.05	2.04	2.06	2.09	2.00	2.24	1.96	2.05	2.04	2.01	2.09
Total	100.38	100.72	100.30	100.39	100.37	100.24	100.39	100.44	100.51	100.52	101.20
CaO+Na ₂ O	5.1	4.8	6.0	6.7	6.6	5.7	8.1	6.1	6.0	5.9	3.4
Log(Fe ₂ O ₃ /K ₂ O)	0.52	0.62	0.49	0.45	0.51	0.50	0.55	0.60	0.59	1.30	1.24
Log(SiO ₂ / Al ₂ O ₃)	0.40	0.40	0.37	0.34	0.35	0.41	0.29	0.42	0.30	0.37	0.34
CIA	78.05	77.47	75.29	73.35	72.66	74.17	72.38	73.76	78.11	78.62	86.04
FeO	4.94	7.52	5.69	6.27	7.64	6.47	6.83	6.68	5.84	9.07	9.48
DF1	-7.48	-11.48	-9.37	-10.56	-13.07	-10.75	-10.94	-10.31	-9.07	-10.54	-9.75
DF2	5.36	3.76	6.01	6.13	5.87	5.74	7.05	5.75	5.66	5.33	3.88

3.3. Lithochemical characterization of XFR analysis data

In this section, we used the different concentrations of elements (major and trace) recorded in Table3. to produce geochemical diagrams, with the aim of providing additional information to the results obtained from petrographic observations. To highlight the petrogeochemical characteristics of the Kodiarani rock formations [20].

The lithomodeller software (GCDKit) was used for the statistical processing of the data. At the end of this processing, five (5) diagrams were obtained, namely: The Tarney 1977 diagram, the Heron 1988 diagram, the A-CN-K and CIA diagram of Fedo, the K₂O/Na₂O versus SiO₂ diagram of and the DF1 versus DF2 diagram of Bhatia (1983).

In Tarney's 1977 diagram, the TiO₂ versus SiO₂ classification scheme shows that all the samples analyzed are SiO₂-rich with a low TiO₂ concentration. These samples fall into the sedimentary rock category.

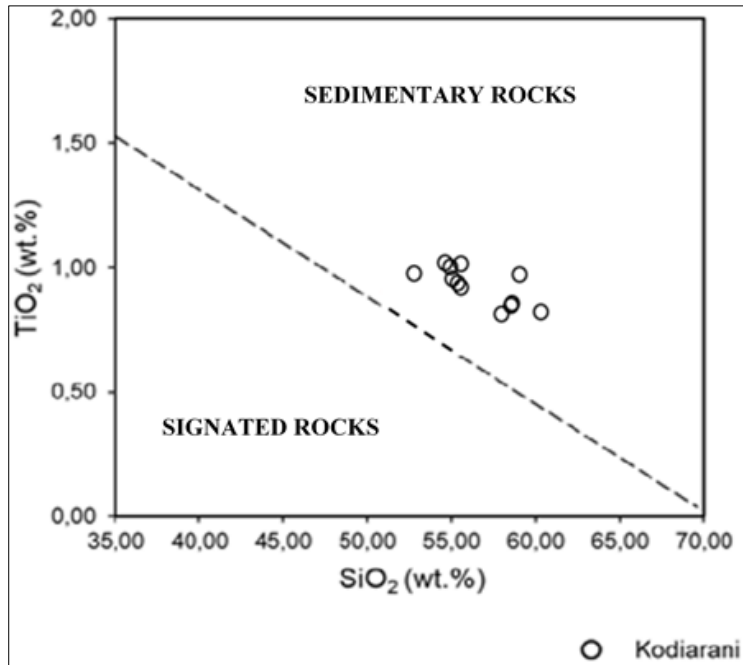


Figure 7 Positioning of meta-sediment samples from the Kodiarani sectors in the TiO₂ versus SiO₂ diagram

Using Herron's (1988) discrimination diagram based on $\text{Log} (\text{Fe}_2\text{O}_3 / \text{K}_2\text{O})$ versus $\text{Log} \text{SiO}_2 / \text{Al}_2\text{O}_3$. The analysis showed a low $\text{SiO}_2 / \text{Al}_2\text{O}_3$ and $\text{Fe}_2\text{O}_3 / \text{K}_2\text{O}$ content. The majority of the samples are located in shales or schists (sometimes rich in iron) (Fig. 8). This leads us to deduce that the rocks studied are schistose meta-sediments.

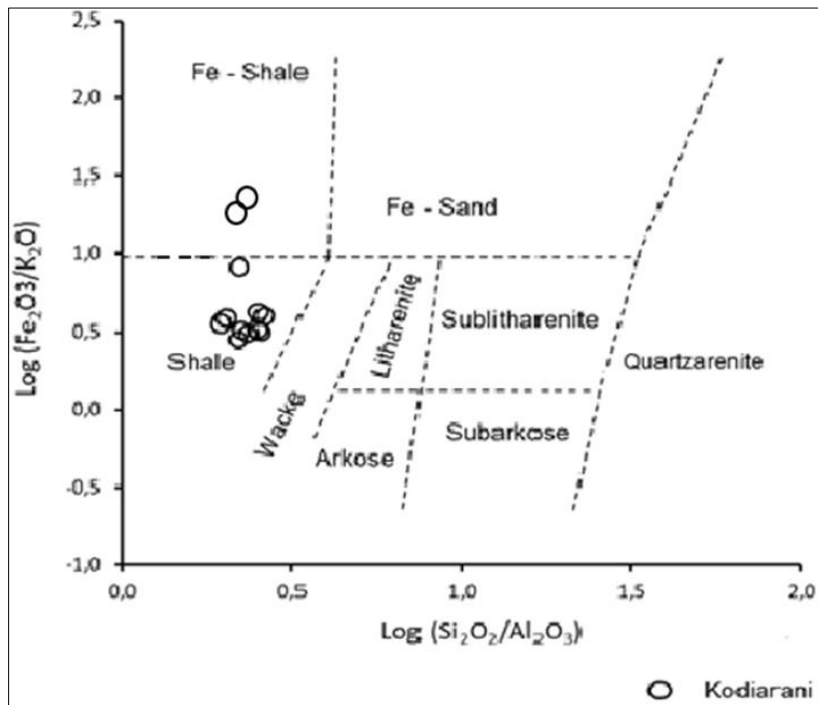


Figure 8 Positioning of meta-sediment samples from the Kodiarani sectors in the diagram) $\text{Log} (\text{Na}_2\text{O} / \text{K}_2\text{O})$ versus $\text{Log} (\text{SiO}_2 / \text{Al}_2\text{O}_3)$

The degree of alteration of the meta-sediment precursor is assessed using the chemical alteration index (CIA): $\text{CIA} = 100 * [\text{Al}_2\text{O}_3 / (\text{Al}_2\text{O}_3 + \text{CaO}^* + \text{Na}_2\text{O} + \text{K}_2\text{O})]$.

For example, the intensity of weathering and the nature of the original sediments were indicated by the A-CN-K and CIA ternary diagrams. Rocks with CIA values > 92 are strongly altered due to the transformation of feldspars into clay minerals. Rocks with CIA values between 60 and 80 with atmospheric alteration and CIA < 60 show little or no alteration.

Thus, our samples plotted in the triangle (fig. 9) with CIA values between 70.62 and 86.04 are in the intermediate alteration range and prove that the meta-sediments in the Kodiarani sector come from andesite and basalt. It should be noted that some of the meta-sediments are rich in smectite.

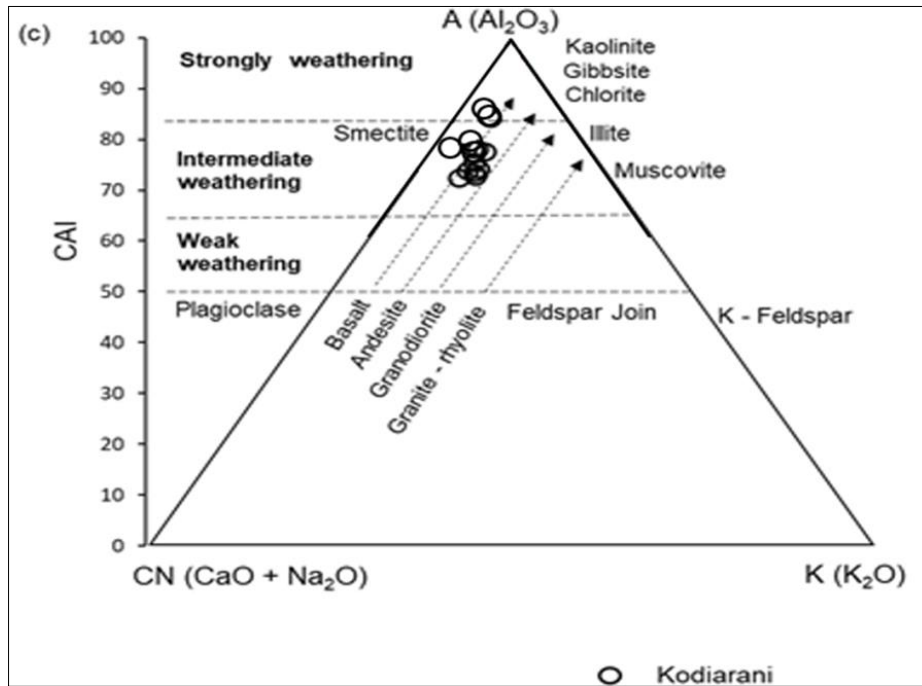


Figure 9 Positioning of the meta-sediment samples from the Kodiarani sectors in the A-CN-K and CIA diagrams

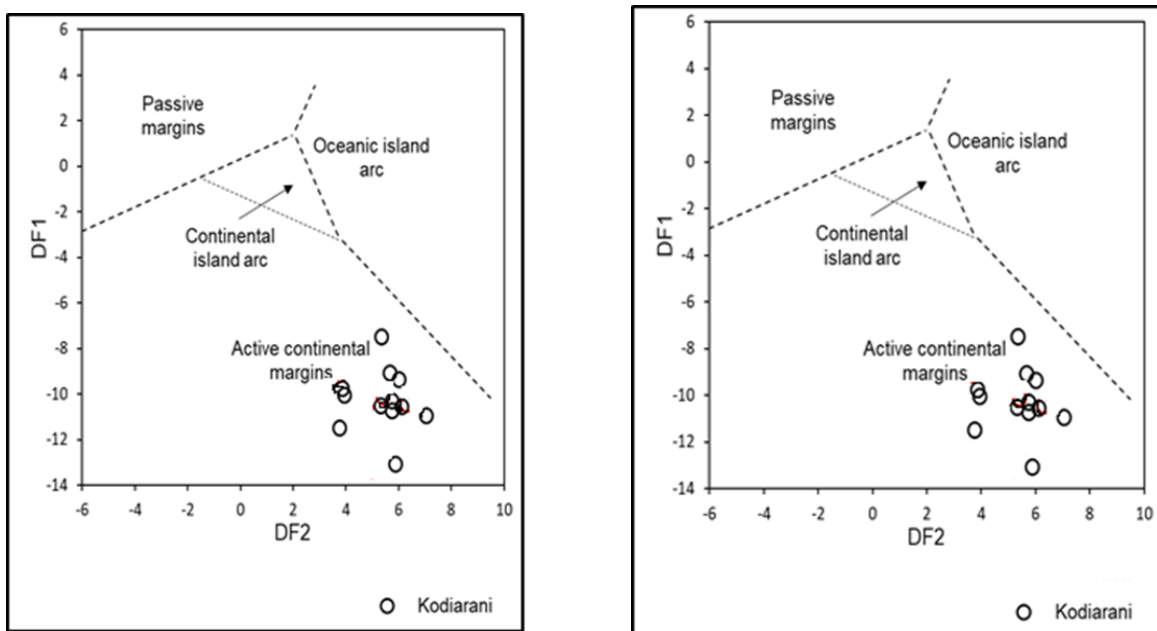


Figure 10 Left Positioning of meta-sediment samples from the Kodiarani sectors in the K₂O/Na₂O versus SiO₂ diagram of Roser and Korsch 1986. Right: Positioning of meta-sediment samples from the Kodiarani sectors in the DF1 versus DF2 diagram

To get an idea of the geodynamic depositional environment of the rocks (andesite and basalt) that led to the formation of the meta-sediments, we used the diagrams of Roser and Korsch 1986 and the diagram of Bhatia 1983. The meta-sediments analyzed fall into two domains: the domain of oceanic island arcs and the domain of active continental margins. However, the Roser and Korsch diagram shown in Fig. 10 indicates that the meta-sediments belong to the domain of oceanic island arcs [22, 23].

$$[DF1 = -0.421SiO_2 + 1.988TiO_2 - 0.526Al_2O_3 - 0.551Fe_2O_3 - 1.610FeO + 2.720MnO + 0.881MgO - 0.907CaO - 0.177Na_2O - 1.840K_2O + 7.244P_2O_5 + 43.57.]$$

$$DF2 = - 0.0447SiO_2 - 0.972TiO_2 + 0.008Al_2O_3 - 0.267Fe_2O_3 + 0.208FeO - 3.082MnO + 0.140MgO + 0.195CaO + 0.719Na_2O - 0.032K_2O + 7.510P_2O_5 + 0.303].$$

It should be noted that the Tarney diagram confirms the results obtained from macroscopic observations of the facies described above, indicating that the rocks studied are sedimentary. However, the diagrams of Heron 1988 and Fedo et al. 1995 support a slight difference. According to Heron's diagram, the samples are mainly schists (sometimes with iron). The data from this diagram suggest that the meta-sediments composed of schists derive from the erosion of andesite's and basalts. These rocks were emplaced in a tectonic environment of active continental margins and/or oceanic island arcs [23].

4. Conclusion

The search for gold is a recurring problem in Birimien formations, particularly in the greenstone belts of West Africa, where few studies have been carried out on this issue.

- TOROGOLD's exploration work in Doko (Siguiro prefecture) in Guinea has helped to address this problem. This work led to the identification of the Kodiarani prospect. Analysis of the geochemical data revealed the existence of two types of gold mineralization: disseminated, observed throughout the lithology, and vein-type, characterized by the emplacement of quartz veins.
- The mineralized zones are hosted in meta-sediments (schists) impregnated mainly by supergene alteration.
- They are marked by strong haematization and quartz veins coinciding with high gold grades. This distribution of gold (vein-type and disseminated) was mentioned on the Kourouba Licence, where dissemination of gold in rocks is identified as the dominant type. This explains why it is controlled by the lithology. These deposits are generally linked to the hydrothermal alteration that would have induced these two (2) types.
- Following our petrographic observations of the various samples collected in the field (chip-tray) combined with the results of geochemical analyses, we identified the meta-sediments as host rocks represented by shales, emplaced in an environment of oceanic island arc and active continental margin. The basaltic and andesitic source of our samples is consistent with the juvenile nature of the Birimien formations. The results of this study have enabled us to reassure ourselves of the existence of gold in this region.

Compliance with ethical standards

Acknowledgments

I would like to express my sincere thanks to the people of good will who contributed to the production of this document. I solemnly thank Dr Ahmed Amara KONATE for his guidance and advice in writing scientific documents of this kind, despite his many duties. I would also like to thank Mr. Kandas Keita, a doctoral student at the Institute National Polytechnique Félix Houphouët Boigny in Yamoussoukro, for his criticism and amendments to the drafting; and Mr. Mamadou Oury Diallo, a geological engineer and doctoral student at the Institute National Polytechnique Félix Houphouët Boigny in Yamoussoukro, for his unconditional contribution and translation of this document.

Disclosure of conflict of interest

The authors unanimously find no obstacle to the submission of this article to this journal.

The research that led to these results was funded by the General Management of the Institute Superior des Mines et Geology de Boké and the Centre Emergent Mines et Society.

References

- [1] Bonhomme, M., 1962. Contribution to the geochronological study of the West African platform. Clermont-Ferrand. 62p
- [2] BCEOM and ORSTOM, 1992. Hydrological Assessment of Sub-Saharan Africa, West African Countries. 55p
- [3] Bessoles, B., 1997. Geology of Africa, The West African Craton 403.
- [4] Cavanagh et al, 1987. Geological, lithogeochemical and humus survey on the Bourbeau property .25p.
- [5] DIOP. M. Here are the five (5) largest new gold producers in Africa. (2019). [Online]. Available at: <https://afrique.le360.ma/autre-pays/economie/2019/05/07/26316>.
- [6] DELAMOU. T.A., 2011. Application and usefulness of mapping in the Sintroko gold mines - SAG concession (Siguiiri) (Graduate thesis). Higher Institute of Mines and Geology of Boké. 58p
- [7] DIALLO, A.B., DIALLO, S., DIALLO, A., LACOMBE, A., 1999. Geological mapping project for the North-East of the Republic of Guinea. 1st Edition. 25p
- [8] KOUAME. K. J. A and FENG. Y. (2015). Research on key issues in the mining industry of Côte d'Ivoire. Don J Geo Min Res, 1(3),035-041.
- [9] Kankan Regional Directorate of Environment, Water and Forests, 2016. Management plan for the protected gallery forest “böötou” in the rural commune of Niandankoro prefecture of Siguiiri. 311p
- [10] KONATE Bintou, N.E. Wandan, K. René Dongo, KOUROUMA Mory, S. A. Boukari (2023), IJSRM. Impact study of the Kiniéro gold mine (SEMAFO) on groundwater and surface water in Guinea. 64-79
- [11] Garant, 2013. "Lithogeochemical characterization of hydrothermal alteration in the southern part of the B1 gold zone at the Meadowbank mine" (Thesis).
- [12] Goloubinow, R., Nickles, M., 1948. Geological map at 1:500,000 and Explanatory Notes on the Kankan sheets – West and East. Dakar
- [13] Jérôme, A., 2017. “Studies of gold mineralization in the Mana-Burkina Faso district. Hydrothermal evolution of a gold system and tectonometamorphic constraints” (Master’s thesis). University of Quebec at Chicoutimi. 207p
- [14] Diallo. M.C., Tall. A and Traoré. L. The challenges of governance of the mining sector in Guinea. (2011).136. [Online]. Available at: <https://icsid.worldbank.org>.
- [15] CAMARA. S and BANGOURA. A. (2017). The development of water resources in Guinea for economic, social and sustainable development. J Wat Env Sci, 1(22), 106-114.
- [16] Koffi et al, 2018. Petrographic and geochemical characteristics of the meta-sediments of the South-Eastern part of the Comoé basin (North of Alépé South-East of Ivory Coast). Ivory Coast.67p.
- [17] KOUAMELAN, A., 1996. Fluid immiscibility and gold deposition in the Birimien quartz veins of the Angovia deposit (Yaouré, Ivory Coast. Univ. Rennes), 1, 263 p.
- [18] YAPI. Y., DONGUI. B., Trokourey. A., Barima. Y., Essis. Y., and Etheba. P. (2014) Assessment of metal pollution in groundwater and surface water in a gold mining environment in Hiré (Ivory Coast). Int J Bio Chem Sc, 8(3), 1281-1289.
- [19] MARMI, R., 2020. Geochemistry-Prospecting; chemistry course-L3_S6 GRM, Department of Geological Services in Nancy (France). 25p.
- [20] OBERTHUR, T., Schmidt, M.A., Vetter, U., Simon, K., Amanor, J.A., 1996. Gold mineralization in the Ashanti belt of Ghana: genetic constraints of the stable isotope geochemistry. Econ. Geol. 45p.
- [21] PERRAULT, 1987. Distribution of gold in the host rocks of gold deposits in the Lamaque-New Pascalis-District region of Val-D’or. 30p.
- [22] Yao. K. A. F. (2018). Development of a methodology for a better assessment of the environmental impacts of the extractive industry. phdthesis. 261. [Online]. Available at: <https://tel.archives-open.fr/tel-01748054>.
- [23] Sycamore mining. Environmental and social impact study of the Kiniéro gold mine in Guinea. (2020), report. 150p.